Journal of the Brazilian Society of Mechanical Sciences and Engineering (2021) 43:184
https://doi.org/10.1007/s40430-021-02893-x

TECHNICAL PAPER

Energy, exergy and exergoenvironmental (3E) analyses of power plant integrated with heliostats solar field

Eduardo J. C. Cavalcanti[1] · **Jonathan L. B. Azevedo**[1]

Received: 22 July 2020 / Accepted: 12 February 2021 / Published online: 7 March 2021

Abstract
This paper analyzes a solar tower power plant driven by a heliostat solar field, which has no fuel consumption. Exergy and exergoenvironmental assessments are utilized to evaluate the sustainability of power, based on the Eco-Indicator 99 method. This solar system does not burn fuel, and therefore there is no generation of greenhouse gases (GHG) due to combustion. The direct normal irradiance per hour was considered to evaluate the performance of the plant. The results indicate that the heliostat field and solar receptor present the highest exergy destruction rates and are responsible for the highest environmental burden of plant. The worst components from an exergoenvironmental perspective were identified. The best case of the solar tower power plant considers a daily operation of 12 h. This condition produced the lowest specific environmental impact of electricity (0.543 mPt/kWh) and the highest exergy efficiency, 18.89%. However, this condition led to the highest environmental impact rate for components, 55.99 Pt/h, due to the net power of 104.69 MW. When the system operates for 24 h per day, the specific environmental impact of electricity is 0.95 mPt/kWh. The results are compared with the literature data. The effect of the energy storage system reduced the net power and increased the amount of molten salts. The environmental impact rate associated with components and total environmental impact rate have a dominant effect on the environmental performance of the plant. A sensitivity analysis showed the effect of operation time, which reduces exergy efficiency and increases the specific environmental impact of electricity.

Keywords Exergy · Exergoenvironmental analysis · Heliostats · Solar field · Tower power plant

List of symbols

A	Area
B	Specific environmental impact or average environmental impact per exergy unit
$\dot{B}$	Environmental impact rate
$\dot{B}_D$	Environmental impact rate related to exergy destruction
$\dot{E}$	Exergy rate
f_b	Exergoenvironmental factor
n	Number
n_y	The years number of component's operation
n_h	Number of hours per years
r_b	Relative environmental impact difference
$\dot{Y}$	Environmental impact related to the component
Y	Environmental impact of component during the life cycle

Abbreviations

ARS	Absorption refrigeration system
CCHP	Cooling, heating and power
CCS	Carbon capture and storage
CO_2	Carbon dioxide
COND	Condenser
CRF	Capital recovery factor
CT	Cool tank
DEA	Deaerator
DNI	Direct normal irradiation
EI	Environmental impact
EI-99	Eco-Indicator 99
EVA	Evaporator
FW	Feed water
G	Generator
GHG	Greenhouse gases
HT	Heat tank

Technical Editor: Monica Carvalho.

✉ Eduardo J. C. Cavalcanti
educanti@gmail.com

Jonathan L. B. Azevedo
jonathanleandrobrandodeazevedo@gmail.com

[1] UFRN - Federal University of Rio Grande do Norte, Natal, Brazil

HPT	High-pressure turbine
HRSG	Heater recovery steam generator
LCA	Life cycle assessment
LPT	Low-pressure turbine
ORC	Organic Rankine cycle
PH	Preheater
R	Receptor
RH	Reheater
SF	Solar field
SH	Superheater
SPECO	Specific exergy costing
STPP	Solar tower power plant

Subscripts and superscripts

att	Atmospheric attenuation
cos	Cosine effect
D	Destruction
e	Electricity
F	Fuel
field	Heliostats field
helio	Heliostat
int	Interception
ms	Molten salt
P	Product
PF	Pollutant formation
ref	Reflectivity
s&b	Shading and blocking

Greek symbols

ε	Exergy efficiency
η	Efficiency
Δh	Enthalpy variation
φ	Maintenance factor

1 Introduction

Thermal power plants mainly employ fossil fuels, which can be replaced by alternative fuels such as natural gas, ethanol, biofuel and even solar energy, to generate low-carbon energy. Equatorial countries present high solar potential throughout the year, with the highest energy availability and the lowest inter-annual variability of direct normal irradiation (DNI).

Studies related to electricity production using renewable energy have been conducted and demonstrated that even if 100% of operational carbon emissions from power plants are captured, there are still emissions associated with fossil fuel extraction, transportation and preparation [1]. The environmental impacts associated with the consumption of fuel is composed of the fuel production process and the formation of pollutants. Recent research has focused on the reduction in these loads. The environmental burden of pollutant formation can be reduced by using carbon capture and storage (CCS) systems in natural gas power plants [2]. Carbon emissions are separated from exhaust gases, with a reduction in net power. Another possibility is tackling the reduction in impacts related to fuel production. Conventional, fossil fuels have a high environmental burden and the replacement with renewable resources can lead to a decrease in impacts, such as the use of eucalyptus biomass, which reduced the specific environmental impact of electricity [3]. The environmental impacts due to fuel production were reduced although overall emissions increased.

The use of solar resource to replace conventional fuel has gained importance, and optimization studies have demonstrated that this technology is even more attractive from economic and environmental viewpoints. Dish Stirling and photovoltaic facilities were compared using the Eco-Indicator 99 and CML2 methods [4], with indicators in terms of CO_2-eq emissions and millipoints, respectively. For higher capacities, solar energy concentration power plants with solar towers present some of the highest efficiencies regarding power production [5]. Solar towers can lead to performance improvements and cost reductions due to technology innovations in the solar components. Some of the advantages of solar tower systems include high temperatures, high thermal efficiencies and the possibility of integration with other power cycles. The steam generator was optimized in an economic study, regarding a 110 MWe solar power tower plant [6], and the results showed that the optimum pinch point temperature differences were very close to 2.6 °C and 3 °C.

Exergy analysis is a useful approach, which distinguishes the quality of energy and helps assess and compare processes rationally and meaningfully. It can assist in improving and optimizing designs and analysis by identifying the causes and locations of irreversibility [7]. A closed Brayton cycle-based combined cycle for solar power tower plants was studied using energy and exergy evaluations [8], concluding that the solar field was responsible for the greatest losses of energy and exergy destruction. The influence of solar parameters is more significant than power block parameters. A solar system with supercritical CO_2 as the heat transfer fluid in the receiver (instead of atmospheric air) was presented by [9], which determined that the receiver and condenser are the main sources of exergy destruction.

Exergy and economic evaluations were developed for a coal power plant with and without a solar tower field [10], concluding that the hybrid plant emits fewer pollutants, decreases fuel consumption and was also able to increase exergy efficiency. The effect of the steam generation of a solar tower plant was studied by [11], where maximum exergy efficiency was achieved manipulating the pinch point temperature difference in the heat exchangers. The results showed that the solar receptor, the condenser and the thermal storage system are the components with highest exergy destruction rates. A new integrated solar tower system was developed by adding a multistage flash distillation subsystem [12], producing power and freshwater. The results of the exergy analysis determined the solar field as the main source of exergy destruction, followed by the steam generator. Solar integration within a combined cycle gas turbine was evaluated [13], which added supplementary heat to evaporators and compared the results with conventional combined cycle gas turbine systems. Different configurations of solar organic flash cycles were optimized to find the most efficient configuration and optimum flashing temperature [14]. A comparison of three trigeneration systems, which integrated a power plant with a solar subsystem, a biomass subsystem and a solid oxide full cell subsystem, was carried out by [15], using a DNI value of 800 W/m^2. The results revealed an increase in exergy efficiency for all systems. The integration with solar subsystem showed the smallest increase in efficiency, and the solar subsystem presented minimum CO_2 emissions. New applications based on exergy analysis can be found in [16–18]. Parabolic troughs and solar towers were combined in a 660 MWe coal-fired power generation system [16], where the solar fields increased fuel savings and reduced coal consumption. The use of solar towers in a multigeneration system for the production of power, heating, cooling, drying, and hydrogen generation and liquefaction was studied by [17], with energy and exergy efficiencies evaluated as 60.14% and 58.37%, respectively. The solar tower subsystem presents the highest exergy destruction, and the most critical parameters are solar radiation and pinch point temperature of HRSG. The performance of a solar tower power plant (STPP) cooled by water (wet cooling mode) and cooled by air (dry cooling mode) was investigated by [18]. The dry cooling mode presented lower energy and exergy efficiencies and higher investment cost. However, the dry cooling system reduces its annual water consumption by almost 94.40%.

Regarding exergoenviromental analysis, it is similar to exergoeconomics, which associates an economic indicator with exergy flows. The aim of exergoeconomic analysis is to minimize the cost rate per exergy of product [7]. Exergoenvironmental analysis associates the exergy rate with an environmental indicator, such as the Eco-Indicator 99, to understand the formation process of environmental impacts. Its methodology was developed by [19] and takes into account the life cycle assessment of all components. There are many applications, with the objective of evaluating the environmental impact rate per exergy unit of product. However, for the specific case of solar field, there are limited studies. A 400 MWe natural gas combined cycle with solar field was studied by exergoeconomic and exergoenvironmental analyses [20], with detailed calculations of the environmental impact of each component. The parabolic trough collector field was able to reduce the environmental impact rate per exergy unit in − 3.9%, due to the increase in power due to the solar field. A similar system with 440 MW [13] was evaluated, and the values of specific exergoeconomic and exergoenvironmental parameters were calculated, demonstrating a reduction in the specific environmental impact of power. An advanced exergoenvironmental analysis of a solar trigeneration energy system was carried out by [21], where flat plat collectors were used for electricity production and operated during 24 h a day at low efficiencies. The system was composed of an organic Rankine cycle (ORC) with R123 and a double-effect LiBr/H_2O absorption refrigeration system (ARS), with 143.5 kW capacity and specific environmental impacts of electricity at 5.08 mPt/kWh. Another trigeneration system [22] was driven by solar and geothermal energy and employed R1234ze, and the capacity and specific environmental impacts of electricity were 11.29 kW and 1221 mPt/kWh, respectively.

The variability of solar irradiance leads to the intermittency of power generation. Variations in electricity tariff and power demand encourage the integration of thermal energy storage (TES) systems within power plants. A cost analysis of thermal energy storage systems integrated with a concentrated solar power plant was studied by [23]. Four systems were modeled considering electricity generation, and technoeconomic performances were assessed. The problems and limitations encountered in an experimental setup were described by [24], where two-tank molten salt TES for solar power plants at pilot scale was investigated for different materials, components and operational strategies. Most studies on TES are based on the performance and economic aspects. Few studies have focused on environmental analyses. A *cradle-to-grave* Life cycle assessment (LCA) was developed for three different TES systems [25]: solid media, molten salt (mixture of NaNO3 and KNO3) and phase change material (PCM). Molten salts are responsible for more than 94% of the environmental loads.

There are no studies on the exergoenvironmental analysis of a purely solar system. The consumption of fossil fuels is the primary source energy of the world; however, it is responsible for pollutant emissions in the atmosphere, causing the global warming and climate change. Renewable technologies for energy generation have been developed with the aim of reducing dependence on these finite fossil resources, decreasing the emissions of pollutants and avoiding greater environmental issues.

This study investigates a 100 MW steam turbine system driven only by a heliostat field. The objective is to evaluate the exergy and exergoenvironmental performance of the solar power plant (which does not consume fuel) along with the formation of pollutants. The effect of thermal tanks was investigated. Solar storage is a critical limitation in solar thermal power plants. Many works have used a high value of DNI in their analysis, leading to an overestimation of solar power plant performance. The variation of DNI throughout the day was taken into account herein, considering an average value of DNI to produce more realistic results. The performance of the storage system was described in detail.

The specific contributions of this study are the development of a model, based on exergy and exergoenvironmental analyses, for steam power plant integrated with a solar field. In addition, the specific environmental impacts of electricity produced were calculated, considering the purely solar system (no fuel combustion) along with the environmental impact factor of all components. The dynamic storage system was considered, and its flow rate of molten salt reflected the variation in irradiance throughout the day. The value of the environmental impact rate per exergy unit of electricity should be minimum. The results of the analyses presented herein can help identify and promote cleaner, low-carbon power systems.

2 Materials and methods

The cycle operates with two steam turbines producing 100 MW, described as follows.

2.1 System description

Solar energy is concentrated from the heliostats field to the receiver of the solar tower. The thermal energy is absorbed by a molten salt mixture, which reaches high temperatures. This energy is transferred to water in heat exchangers, generating steam. A hot tank accumulates hot molten salts during sunlight hours. The molten salt mixture drives the heat exchangers and flows into a cooling tank during the power generation process. The schematic diagram is shown in Fig. 1.

2.2 Energy analysis

Mass and energy balances were developed to develop the mathematical model. The energy balance is based on the first law of thermodynamics, assuming steady-state conditions, except in the hot and cool tanks, and is shown in Eq. 1. Kinetic and potential energy variations were not considered:

$$\dot{Q}_{\mathrm{CV}} + \sum_{\mathrm{in}} \dot{m} \cdot h = \sum_{\mathrm{out}} \dot{m} \cdot h + \dot{W}_{\mathrm{CV}}. \quad (1)$$

The energy balance encompassing the solar field and the receptor is important to evaluate the mass flow rate of molten salt into the receptor. The mass flow rate of molten salt into the receptor, between points 9 and 10, is calculated considering the solar energy rate of heliostat field and its efficiency, as given by Eq. 2.

$$\mathrm{DNI} \cdot n_{\mathrm{helio}} \cdot A_{\mathrm{helio}} \cdot \eta_{\mathrm{field}} \cdot \eta_{\mathrm{r}} = \dot{m}_{\mathrm{ms}} \cdot \Delta h. \quad (2)$$

The temperature conditions of molten salt at points 10 and 11 are 285.50 °C and 565.0 °C, respectively [6].

The following assumptions were considered in the model:

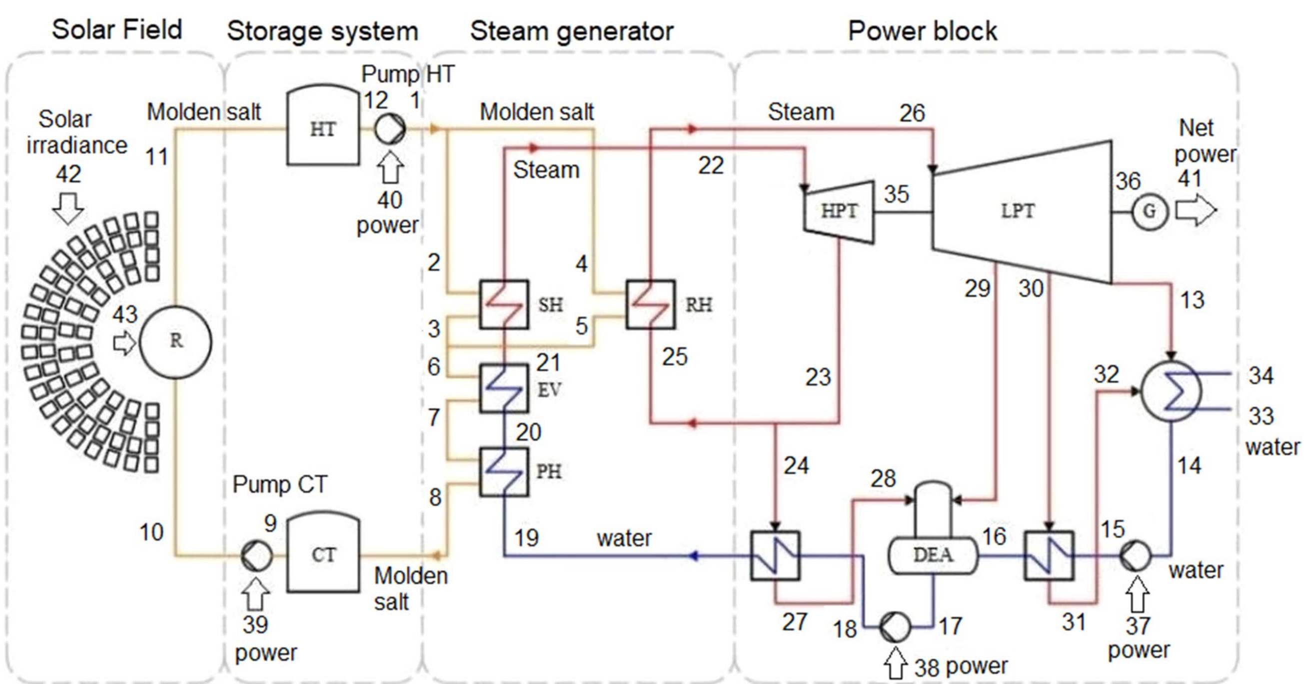

Fig. 1 Schematic representation of cycle. Adapted from [6]

- The dead state is air temperature at 26 °C and atmospheric pressure of 101.325 kPa.
- The flow in heat exchangers is ideal; the components are adiabatic.
- The isentropic efficiencies of molten salt pumps and water pumps are 70% and 80%, respectively.
- The isentropic efficiencies of low- and high- pressure turbines are 90% and 80%, respectively.

The solar field has (n_{helio}) 10,347 heliostats with an area of (A_{helio}) 115.7 m^2. The height of the solar tower is 195 m, according to [11]. The average direct solar radiation considered as reference uses data retrieved for March 21, in Natal (Northeast Brazil), between 11 a.m. and 12 p.m. with direct solar radiation of 846 W/m^2 [26].

The total efficiency of the heliostat field (η_{field}) is the product of all efficiencies related to losses, considering a cosine effect of 0.8267 (η_{cos}), shading and blocking as 0.9698 ($\eta_{s\&b}$), interception as 0.9710 (η_{int}), atmospheric attenuation as 0.9383 (η_{att}) and by reflectivity as 0.88 (η_{ref}), following Eq. 3.

$$\eta_{field} = \eta_{cos} \cdot \eta_{s\&b} \cdot \eta_{int} \cdot \eta_{att} \cdot \eta_{ref}. \tag{3}$$

The total efficiency of the heliostat field is 64.28% [8] and is related to the amount of heat of the sun that actually reaches the receiver. This is considered to be within a good range of heliostat field efficiencies. There are also heat losses in the receiver, referring to a difference in the amount of heat that reaches the receiver and the amount of heat that is actually transferred from the receiver to the flow of molten salt. These losses are related to the efficiency of the solar tower receiver. In the results obtained by [27], the efficiency of the receiver (η_r) changed from 76 to 87% depending on its surface temperature. Herein, the efficiency of the receiver was considered as 87%. The flow of molten salt is stored in a tank to feed the heat exchangers at a constant mass flow rate, at high temperature.

The molten salt is a mixture of two salts (60% NaNO3 and 40% KNO3). The properties of the mixture, such as enthalpy and entropy, were defined following [28].

2.3 Exergy analysis

This work employs the SPecific Exergy COsting (SPECO) methodology [29], which considers the mechanical, thermal and chemical components of exergy and classifies the exergy flow of each component as fuel and product. In productive components, the exergy rates of product $\dot{E}_P$ and fuel $\dot{E}_F$ are defined by considering the desired result produced by the component and the resources expended to generate this result [29]. The product is defined to be the sum of all the exergy values to be considered at the outlet stream plus all the exergy increases between inlet and outlet streams that are in accordance with the purpose of the component. The fuel is defined as all the exergy values to be considered at the inlet stream plus all the exergy decreases between inlet and outlet streams minus all the exergy increases that are not in agreement with the purpose of the component.

The parameters of the exergy destruction rate were calculated [7] by Eq. 4:

$$\dot{E}_D = \dot{E}_F - \dot{E}_P. \tag{4}$$

The exergy efficiency is defined [7] as Eq. 5:

$$\varepsilon = \frac{\dot{E}_P}{\dot{E}_F}. \tag{5}$$

2.4 Exergoenvironmental assessment

The environmental impact rate combines exergy rates with environmental loads. The environmental balance takes into account the environmental impact rate of each stream and the environmental impact, obtained via life cycle assessment (LCA) for each component. The effect of component-related environmental impacts over the lifetime of systems was first considered in [19]. The environmental impact assessment method used to quantify environmental impacts was Eco-Indicator 99 (EI99) [28], which follows the guidelines of international standard approaches—ISO 14040 [30]. Environmental loads can encompass consumed materials, production processes, transportations, heat and electricity consumption, and disposal scenarios. In EI99, environmental impacts are classified into three categories of damage: human health, ecosystem quality and natural resources. Results for each category are quantified and normalized, then weighted and expressed in points (Pt or mPt). One point represents one-thousandth of the annual environmental load of one average European inhabitant [31]. To better understand the environmental burden of emissions (b^{PF}) and electricity generated in two different countries, their parameters are presented in Table 1:

Table 1 Environmental impact of each pollutant emission (b^{PF}) and the electricity from two countries. Source: [31] and [45]

Emissions and electricity	EI-99 index
CO_2	5.45 mPt/kg
CO	8.36 mPt/kg
SO_2	1499.37 mPt/kg
NO	4217.74 mPt/kg
NO_2	2749.36 mPt/kg
1 kWh in Brazil	33.40 mPt/kWh
1 kWh in Greece	105.00 mPt/kWh

The emissions of SO_2, NO_2 and NO are much higher than the emissions of CO_2 and CO. The environmental impact of electricity is associated with different generation sources. The electricity generated in Brazil is lower than the electricity in Greece, because its source is based on hydroelectric plant, when the source of Greece is based on coal and natural gas power plants. The reader is directed to [31] for more details.

In the exergoenvironmental balance based on the SPECO method, the environmental impact rate of product $\left(\dot{B}_{\mathrm{P}}\right)$ is evaluated as given by Eq. 6:

$$\dot{B}_{\mathrm{P}} = \dot{B}_{\mathrm{f}} + \dot{Y} + \dot{B}^{\mathrm{PF}}. \tag{6}$$

The advantage of a 100% solar-driven power plant is that the effect of pollutant formation is null, as there is no combustion. This balance can be shown by Eq. 7, using the average environmental impact per exergy unit of product (b_{P}) and fuel (b_{F}):

$$b_{\mathrm{P}} \cdot \dot{E}_{\mathrm{P}} = b_{\mathrm{F}} \cdot \dot{E}_{\mathrm{F}} + \dot{Y}. \tag{7}$$

The component-related environmental impact rate $\left(\dot{Y}\right)$ is obtained by means of a LCA [19], considering the material composition of equipment. The relationship between different materials and the environmental impact per mass unit is shown [20]. This environmental impact must account for the lifetime of equipment, considering the number of operation years (lifetime, n_{y}) and the number of annual operation hours (n_{h}), according to Eq. 8:

$$\dot{Y} = \frac{Y}{n_{\mathrm{y}} \cdot n_{\mathrm{h}} \cdot 3600}. \tag{8}$$

The lifetime (n_{y}) has been estimated as 25 years, and the number of annual operation hours of operation (n_{h}) r varies for each component: solar system components—heliostats, solar tower receiver, cold molten salt pump—operate for 9 h a day while the other components operate for 24 h a day.

The environmental impact rate related to exergy destruction is evaluated by the average environmental impact per exergy unit of fuel, as expressed by Eq. 9:

$$\dot{B}_D = b_f \cdot \dot{E}_{\mathrm{D}}. \tag{9}$$

It is important to note that in the heliostat field, the environmental impact of exergy destruction should be calculated using the average environmental impact per exergy unit of product, as shown in Eq. 10. Because the environmental impact of solar radiation is null, the average environmental impact per exergy unit of fuel is null.

$$\dot{B}_D = b_p \cdot \dot{E}_D. \tag{10}$$

The relative difference of environmental impacts demonstrates the potential for reducing the component-related impacts in a system [31]:

$$rb = \frac{b_{\mathrm{P}} - b_{\mathrm{F}}}{b_{\mathrm{F}}}. \tag{11}$$

The exergoenvironmental factor indicates the significance of environmental impacts associated with a component, related to the total impacts, as shown in Eq. 12. A low value of this parameter indicates the component with higher environmental impact associated with exergy destruction [31].

$$f_{\mathrm{b}} = \frac{\dot{Y} + \dot{B}^{\mathrm{PF}}}{\dot{Y} + \dot{B}^{\mathrm{PF}} + \dot{B}_{\mathrm{D}}}. \tag{12}$$

Table 2 shows the parameters related to exergoeconomic and exergoenvironmental analyses, for a better understanding of similarities.

Exergoeconomic analysis uses an economic indicator, while the exergoenvironmental analysis works with an environmental indicator. The difference is in the balances, where the exergoenvironmental analysis considers the effect of pollutants emitted. However, in this study there are no emissions associated with pollutant formation because the system

Table 2 Comparison between exergoeconomic and exergoenvironmental analyses

Analysis	Exergoeconomic	Exergoenvironmental
Indicator	Cost (US$)	Environmental (mPt)
Rate	$\dot{C}$(US$/s)	$\dot{B}$(mPt/s)
Specific indicator or indicator rate per exergy unit	c (US$/kJ)	b (mPt/kJ)
Balance	$\dot{C}_{\mathrm{P}} = \dot{C}_{\mathrm{f}} + \dot{Z}$(US$/s)	$\dot{B}_{\mathrm{P}} = \dot{B}_{\mathrm{f}} + \dot{Y} + \dot{B}^{\mathrm{PF}}$(mPt/s)
Rate related to components	$\dot{Z} = \frac{z \cdot \mathrm{CRF} \cdot}{n_{\mathrm{h}} \cdot 3600}\left(\frac{\mathrm{US\$}}{\mathrm{s}}\right)$	$\dot{Y} = \frac{Y}{n_{\mathrm{y}} \cdot n_{\mathrm{h}} \cdot 3600}\left(\frac{\mathrm{mPt}}{\mathrm{s}}\right)$
Rate related to exergy destruction	$\dot{C}_{\mathrm{D}} = c_{\mathrm{f}} \cdot \dot{E}_{\mathrm{D}}$	$\dot{B}_{\mathrm{D}} = b_{\mathrm{f}} \cdot \dot{E}_{\mathrm{D}}$
Relative difference	$r = \frac{c_{\mathrm{P}} - c_{\mathrm{F}}}{c_{\mathrm{F}}}$	$r_{\mathrm{b}} = \frac{b_{\mathrm{P}} - b_{\mathrm{F}}}{b_{\mathrm{F}}}$
Factor	$f = \frac{\dot{Z}}{\dot{Z} + \dot{C}_{\mathrm{D}}}$	$f_b = \frac{\dot{Y} + \dot{B}^{\mathrm{PF}}}{\dot{Y} + \dot{B}^{\mathrm{PF}} + \dot{B}_{\mathrm{D}}}$

is entirely driven by solar resource. Exergoenvironmental analyses are different from the environmental analyses presented by [32], which take into account the cost of pollutant emissions as 24 US$/tonnes of CO_2 emitted [32].

3 Results and discussion

Given the direct solar irradiance (DNI) per hour [26], number of heliostats as 10,347 with an area of 115.7 m^2 and total efficiency of the heliostats field of 64.28%, the sun and receptor energy and mass flow rate of molten salt are presented in Table 3.

The last time of day (16 h) corresponds to the average DNI for the period 16 h to 17 h. Solar data were collected in 2010. As DNI increases, the energy and mass flow rate increase. The average DNI is 493.7 W/m^2. The average sun energy that reaches the heliostat is 591.48 MWh. The average input and output energy at receptor are 379.92 MWh and 288.02 MWh, respectively. The average mass flow rate of molten salt is 659.2 kg/s, which flows into the receptor.

The model of the solar power plant encompassed mass, energy, exergy and exergoenvironmental balances for 24-h operation time. A validation of specific exergy was also carried out. The properties of each state point (Fig. 1) are shown in Table 4.

Temperature and pressure data were collected [6], which led to the determination of mass flow rate, specific exergy (e), exergy rate and environmental balances. A specific exergy value based on a similar solar power plant [11] was included to validate the model. Some data, such as pressure and temperature between both systems, are not the same and indicated as "I" in Table 3. The difference in specific exergy (Δe) changed from -5.99 to 7.56%.

The mass flow rates of molten salt in points 1 to 8 are constant. The model was developed for an average DNI of 0.4937 kW/m^2. The net power produced (point 41) is 52.64 MW of electricity and is composed of the contributions of high- and low-pressure turbines (35 and 36) minus the power of two water pumps (37 and 38) minus the power of two salt molten pumps (39 and 40). The condenser is cooled by water at points 33 and 34, being a dissipative component. This means that the environmental impact rate of point 34 is charged to the four heat exchangers of the Rankine cycle, according to the SPECO approach. The feed water and deaerator outputs are saturate liquids at points 27, 31 and 17. The solar irradiance from the heliostat field has a high exergy rate of 554.12 MW; however, its environmental impact is null. The input receptor at point 43 presents a high environmental impact due to the solar field.

The environmental impact rate per exergy unit of electricity is 264.5 mPt/GJ, and the value of environmental impact rate is 50.12 mPt/h.

Based on Eqs. (4) and (5), the exergy rate destruction and exergy efficiency can be evaluated. Figures 2 and 3 display the exergy rate destruction and exergy efficiency of each component, respectively.

The heliostat solar field (SF) and solar receptor (R) have the highest exergy destruction, due to the high quality of solar energy. (The sun's temperature is around 4500 K.) The temperature is reduced to 1000 K and 600 °C at the surface of the receptor and in the molten salt, respectively. This reduction is the reason for such high exergy destruction [8]. Both solar components account for 97.14% of all exergy destruction. Similar results can be found in [33, 34], where these two components were evaluated and were responsible for 86.83% and 91.08% of all exergy destruction.

The lowest exergy efficiencies are located in the solar receptor (R) and cool salt pump (pump CT). The low solar receptor efficiency is due to the temperature reduction, as previously mentioned. The cool pump works for 9 h, guaranteeing the flow of molten salt. The change in the flow rate of molten salt reduces its efficiency. Because of the composition of the molten salt (60% NaNO3 and 40% KNO3), the

Table 3 DNI per hour, energy per hour and mass flow rate of molten salt

Time of day [h]	DNI [kW/m^2]	$\dot{Q}_{sun}$[kWh]	$\dot{Q}_{rec,in}$[kWh]	$\dot{Q}_{rec,out}$[kWh]	$\dot{m}_{ms}$[kg/s]
7	0.0905	108,354	69,650	52,801	120.8
8	0.3620	433,380	278,575	211,188	483.3
9	0.5585	668,631	429,794	325,827	745.7
10	0.7795	933,189	599,851	454,747	1041.0
11	0.8232	985,504	633,479	480,240	1099.0
12	0.8701	1,046,000	669,539	507,577	1162.0
13	0.7221	864,496	555,696	421,273	964.1
14	0.4130	494,374	317,782	240,911	551.3
15	0.2216	265,336	170,557	129,299	295.9
16	0.0965	115,537	74,267	56,302	128.9
Average	0.4937	591,480	379,919	288,017	659.2

Table 4 Results of balances: exergy rate, specific environmental impact and environmental impact rate

Point	T (°C)	P (kPa)	$\dot{m}$(kg/s)	e (kJ/kg)	e [11] (kJ/kg)	Δe (%)	$\dot{E}$(kW)	b [mPt/GJ]	$\dot{B}$[mPt/h]
1	565.00	1000.0	280.10	374.13	356.94	4.82	104,795	192.9	72,785
2	565.00	1000.0	190.60	374.15	356.93	4.82	71,313	192.9	49,530
3	451.00	1000.0	190.60	260.99	244.16	6.89	49,744	192.9	34,549
4	565.00	1000.0	89.50	374.10	356.95	4.80	33,482	192.9	23,255
5	452.90	1000.0	89.50	262.76	244.30	7.56	23,517	192.9	16,333
6	451.60	1000.0	280.10	261.55	244.21	7.10	73,260	192.9	50,882
7	338.50	1000.0	280.10	161.75	152.39	6.14	45,305	192.9	31,466
8	293.80	1000.0	280.10	126.60	120.26	5.27	35,460	192.9	24,629
9	285.10	150.0	659.20	120.08	113.26	6.02	79,159	524.4	149,437
10	285.50	1000.0	659.20	120.35	117.51	2.42	79,336	524.4	149,787
11	565.00	150.0	659.20	374.09	356.31	4.99	246,600	192.7	171,073
12	564.60	150.0	280.10	373.73	356.32	4.89	104,682	192.7	72,621
13	45.79	10.0	30.31	144.01	153.19	− 5.99	4365	243.8	3831
14	45.79	10.0	32.31	2.82	2.90	− 2.85	91	243.8	80
15	45.93	1510.0	32.31	4.33	4.28	1.25	140	285.1	144
16	80.00	1510.0	32.31	20.33			657	404.2	956
17	198.60	1510.0	42.70	159.70			6819	329.4	8086
18	201.20	12,600.0	42.70	173.65			7415	329.0	8783
19	245.10	12,600.0	42.70	253.44	265.85	− 4.67	10,822	309.5	12,060
20	328.50	12,600.0	42.70	465.78	490.05	− 4.95	19,889	273.7	19,599
21	328.50	12,600.0	42.70	1048.90	1072.93	− 2.24	44,788	252.4	40,696
22	550.00	12,600.0	42.70	1503.54	1535.95	− 2.11	64,201	247.9	57,300
23	371.00	3400.0	42.70	1147.24	1186.25	− 3.29	48,987	247.9	43,721
24	371.00	3400.0	4.04	1146.78	1186.25	− 3.33	4633	247.9	4135
25	371.00	3400.0	38.66	1147.28	1186.25	− 3.29	44,354	247.9	39,586
26	550.00	3400.0	38.66	1389.37	1429.68	− 2.82	53,713	243.8	47,142
27	240.90	3400.0	4.04	238.12			962	247.9	859
28	198.60	1510.0	4.04	231.44			935	247.9	835
29	427.90	1510.0	6.35	1128.66			7167	243.8	6290
30	123.80	100.0	2.00	495.50			991	243.8	870
31	99.61	100.0	2.00				67	243.8	59
32	45.79	10.0	2.00	17.50			35	243.8	31
33	25.00	101.3	632.30				0	0.0	0
34	50.00	101.3	632.30				2626	0.0	0
35	–	–	–				13,585	280.0	13,693
36	–	–	–				39,859	253.7	36,402
37	–	–	–				61	264.5	58
38	–	–	–				683	264.5	651
39	–	–	–				367	264.5	349
40	–	–	–				172	264.5	164
41	–	–	–				52,643	264.5	50,120
42	–	–	–				554,122	0.0	0
43	–	–	–				356,188	15.5	19,919

environmental impact per mass of molten salt is $0.6 \times 377.1 + 0.4 \times 181.7 = 298.9$ mPt/kg [35].

The environmental impact of each component is important in exergoenvironmental analyses. Their values are evaluated based on the weight and the environmental impact per weight unit. Values of mass and environmental impact per mass unit can be found in [3, 17]. Table 5 presents the environmental impacts of the plant components.

The solar system is constituted by a heliostat solar field, solar receptor, two salt pumps and two tanks of molten salts. The steam generator is composed of a superheater, evaporator, preheat and reheater. The power block consists of two

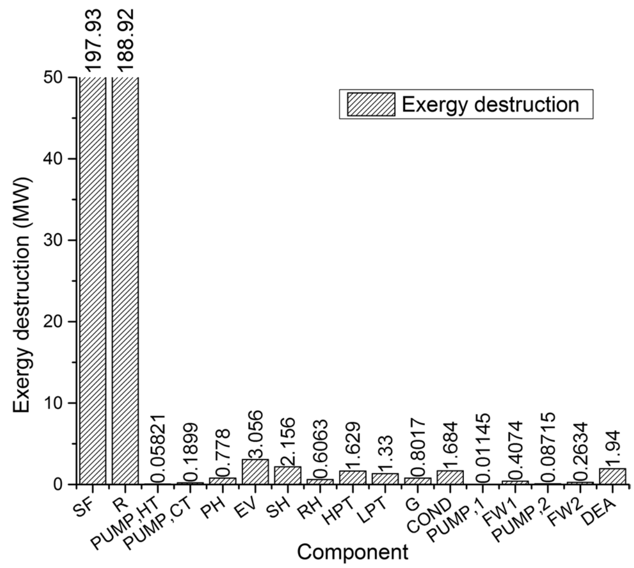

Fig. 2 Exergy rate destruction for each component

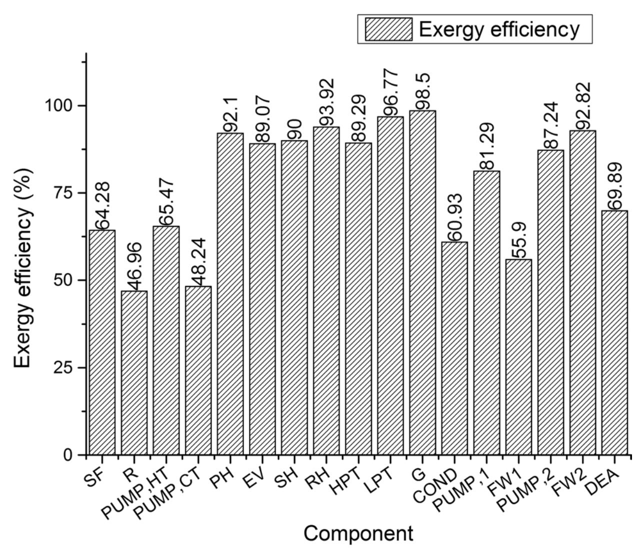

Fig. 3 Exergy efficiency of each component

Table 5 Environmental impacts of plant components

Component group	Y [mPt]	%
Solar system	6.48E+09	96.47
Steam generator	1.62E+08	2.41
Power block	7.53E+07	1.12
Total	6.72E+09	100.00

turbines, generator, condenser, deaerator, two feed water and two water pumps. The solar system has the higher environmental impact, which corresponds to 96% of the overall environmental impact. The molten salt production is the main responsible for this high environmental burden with 4.921 + 09 mPt and 16,461 tonnes, corresponding to 75.9%.

Table 6 shows the environmental impact rate, environmental impact of exergy destruction, average environmental impact per exergy unit of fuel and product, relative environmental impact and exergoenvironmental factor of the different components.

The exergy efficiency and exergy destruction rate have been discussed before. The environmental impact rate was evaluated based on Eq. 9. The solar field and receptor have the highest environmental impact rates. Both components contain an elevated amount of material, such as steel. The average environmental impact per exergy unit of fuel and product is calculated by Eqs. 7 and 8. The four pumps have the highest average environmental impact per exergy unit of fuel, because electricity drives all pumps.

The pumps and feed water 1 have the highest average environmental impact per exergy unit of product. The pump and feed water product are the increase in pressure and the increase in water temperature, respectively. Both products have a low increase in exergy, which leads to a high average environmental impact per exergy unit of product. Similar results were verified by [3], in which the feed water and pump had the higher average environmental impact per exergy of product. The solar field and receptor have the highest values of environmental impact rate related to exergy destruction, because these components have the highest exergy destruction rates.

Calculations of the relative difference of environmental impacts are based on Eq. 12. The highest values were determined for the receptor and pump of the cooling tank. These components present a high potential for the reduction in average environmental impact per exergy unit of product. The solar field has a null value of environmental impact per exergy unit of product, because it is driven by solar irradiance and it has no environmental impacts associated. Regarding the exergoenvironmental factor, both pumps of molten salt present the lowest values, indicating that an increase in their efficiencies can reduce the environmental impact associated with exergy destruction and consequently reduce the specific environmental impact of electricity. The condenser is a dissipative component, whose function is to destroy exergy and should not be modified.

The results of the specific environmental impacts obtained herein were compared with the literature data for systems operating with solar energy. All systems produce electricity and do not burn or emit pollutants. The power, exergy efficiency, time of operation, description of system, environmental impact rate of component, total environmental impact rate and specific environmental impact of electricity are shown in Table 7.

Table 6 Exergoenvironmental parameters

Component	ε[%]	$\dot{E}_D$[MW]	$\dot{Y}$[mPt/h]	B_f [mPt/GJ]	b_p [mPt/GJ]	$\dot{B}D$[mPt/h]	r_b [%]	f_b [%]
SF	64.28	197.93	19,919.00	0.00	15.53	11,069.0	0.00	64.28
R	46.96	188.92	1367.00	15.53	35.35	10,565.0	127.60	11.46
Pump, HT	65.47	0.06	0.02	264.50	404.00	56.5	52.75	0.03
Pump, CT	48.24	0.19	0.10	264.50	548.40	180.8	107.30	0.05
PH	92.10	0.78	8.85	192.90	231.00	540.4	19.72	1.61
EVA	89.07	3.06	29.29	192.90	235.40	2123.0	21.99	1.36
SH	90.00	2.16	620.50	192.90	237.60	1498.0	23.15	29.30
RH	93.92	0.61	197.80	192.90	224.30	421.1	16.24	31.96
HPT	89.29	1.63	114.00	247.90	280.00	1454.0	12.93	7.27
LPT	96.77	1.33	251.50	243.80	253.70	1167.0	4.06	17.73
G	98.50	0.80	25.06	260.40	264.50	751.4	1.57	3.23
COND	60.93	1.68	0.69	243.80	400.20	1478.0	64.15	0.05
Pump1	81.29	0.01	0.21	264.50	360.40	10.9	36.26	1.91
FW1	55.90	0.41	0.92	243.80	436.60	357.6	79.08	0.26
Pump2	87.24	0.09	0.07	264.50	324.70	83.0	22.76	0.09
FW2	92.82	0.26	1.43	247.90	267.20	235.1	7.78	0.60
DEA	69.89	1.94	5.12	222.30	318.50	1553.0	43.23	0.33

Table 7 Comparison of results: specific environmental impact of electricity

Reference	Power [MW]	Exergy efficiency ε [%]	Years/operation hour per year	System description	$\dot{Y}$[mPt/h]	$\dot{Y}+\dot{B}_D$[mPt/h]	b_e [mPt/kWh]
Boyaghchi, Chavoshi [22]	0.01	2.40	15/7446	Solar + Geot + CCHP	32,970.0	69,919.0	1220.00
Montazerinejad et al. [21]	0.14	n.a	20/7446	Solar + OCR + ABS	120.6	12,375.4	5.08
This work with 12 h	104.69	18.89	25/4000	Solar + Rank	55,999.3	101,528.8	0.54
This work with 24 h	52.16	9.41	25/8000	Solar + Rank	48,898.6	150,579.4	0.95

na not available

Boyaghchi and Chavoshi [22] studied a solar–geothermal trigeneration system, producing 11.29 kW of electricity, with 24-h operation, using R1234ze with low efficiency. The solar collector is the flat plate type. The environmental impact rate of all components is 32,970 mPt/h. When this value is combined with the environmental impact rate of exergy destruction, the total environmental impact rate increases to 69,919 mPt/h. [22] presents the highest specific environmental impact of electricity as 1,220.0 mPt/kWh due to the high environmental burden associated with the construction of the system. The environmental impact rate has not been disaggregated per component of the solar–geothermal system.

Mantazerinejad et al. [21] proposed an energy system composed of a solar collector subsystem, an ORC subsystem and a double-effect LiBr/H2O ARS. The net electricity produced is 143.5 kW throughout a 24-h period. The exergy efficiency is not reported. The environmental impact rate of all components (120.6 mPt/h) and the value of total environmental impact rate (12,375 mPt/h) are lower than [22]. Consequently, the specific environmental impact of electricity of 5.08 mPt/kWh is lower. The longer annual operation hours (7446 h) [21, 22] leads to lower power due to low power of steam turbine.

As the total environmental impact rate is reduced, the specific environmental impact of electricity decreases. Many works have demonstrated the high effects of fuel consumption on the specific environmental impact of electricity [3, 16, 36]. The effect of pollutant formation was predominant in [3, 16], where biomass and coal were used. The effects of fuel consumption and pollutant formation changed [36], when different diesel–biodiesel blends were used. However, the system presented herein has no fuel consumption, and therefore environmental impact rate of components and the total environmental impact rates are predominant in the calculation of the specific environmental impacts of electricity.

This work has compared two operation periods: 12 and 24 h a day. As the operation time is increased, power and exergy efficiency decrease. The power dropped from

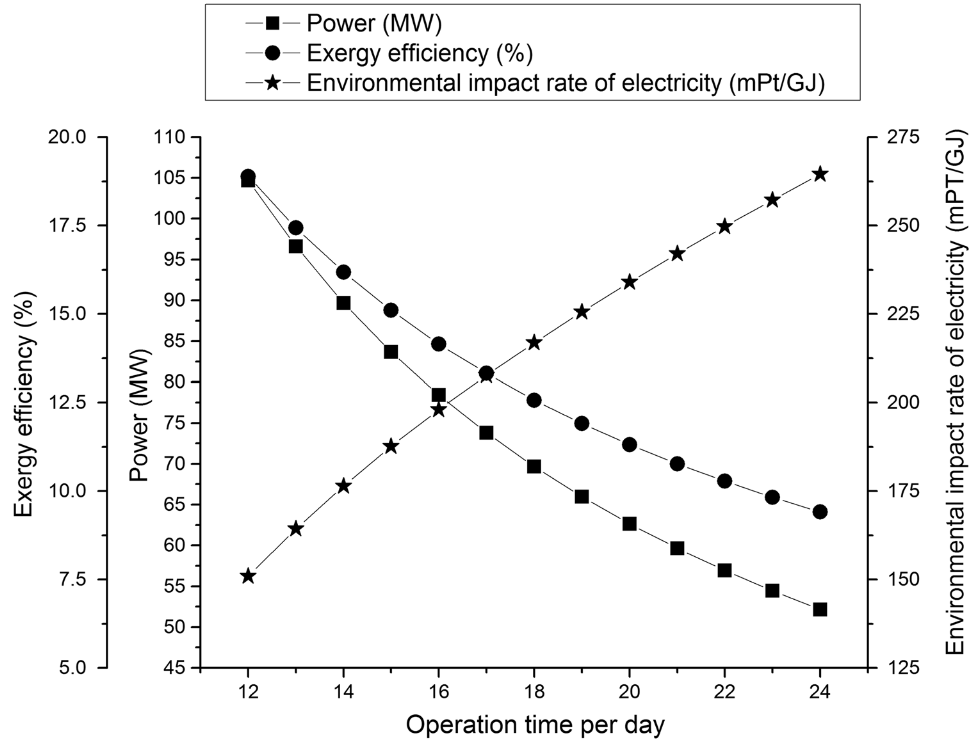

Fig. 4 Effect of operation time on performance

104.69 to 52.15 MW, and the exergy efficiency changed from 18.89 to 9.41%. The environmental impact rate of all components reduced from 55.99 to 48.89 mPt/h, as operation time increases. The capacity of the steam turbine is reduced, leading to an increase in the storage system. The total environmental impact rate increased significantly for 24 h (150.58 mPt/h), due to the lower exergy efficiency and higher environmental impact rate related to exergy destruction. The total environmental impact rate of all components corresponds to 32.48% (48.89/150.5) of the overall environmental impact rate. When the system operates for 12 h, this ratio is 55.15% (55.99/101.52), indicating that the environmental impact rate related to exergy destruction is lower in relation to the 24-h operation period, due to higher exergy efficiency.

The specific environmental impact of electricity is lower for the 12-h operation period, because of the higher value of net power and lower value of total environmental impact rate. The minimum specific environmental impact of electricity occurs when operation time is 12 h a day, at 0.54 mPt/kWh. The reduction in molten salt from 16,463 to 9403 influenced the lower value. In the literature, it is possible to find lower values of specific environmental impact of electricity, such as in [37], where electricity and biofertilizer were produced in a genset-coupled anaerobic digestion plant fed with organic municipal solid waste. The specific environmental impact of electricity is 0.04 mPt/kWh (11.10 mPt/GJ), but the formation of pollutants was not considered.

For a better understanding of the effect of operation time on the specific environmental impact of electricity, a sensitivity analysis was carried out. Figure 4 indicates the exergy efficiency, net power and specific environmental impact of electricity for different operation times.

When operation time changes from 12 to 24 h, the net power reduced from 104.69 to 52.16 MW and the exergy efficiency reduced from 18.89 to 9.41%. As operation time increases, both power and exergy efficiency decrease. In conditions of high operation times, less net power is produced. This happens due to a reduction in the flow of molten salt, and less energy being transferred to steam, which flows into the steam turbine. Less axis power is converted into electricity in the generator.

The operation time of 24 h produces electricity always in a steady-state condition. However, the 12-h operation period increases molten salt flow, net power and exergy efficiency. The system operates in steady-state conditions during the 12 operation hours and is off otherwise.

The specific environmental impact of electricity changes from 0.543 mPt/kWh (150.9 mPt/GJ) to 0.952 mPt/kWh (264.5 mPt/GJ). The longer operation time indicates an increase in the total environmental impact rate of Table 5, due to low exergy efficiency. Additionally, the reduction in net power causes an increment in the specific environmental impact of electricity.

4 Conclusion

A power plant integrated with a heliostat solar field is modeled based on exergy and exergoenvironmental analyses. The effects of direct normal irradiance per hour on the heliostat field and mass flow rate of molten salt into the receptor were shown. Exergy and exergoenvironmental balances were carried out, and the heliostat field and solar receptor present the highest environmental burden within the plant, due to their material composition. These components have the highest environmental impact rate associated with exergy destruction. The pumps of molten salt present the lowest environmental performances. The specific environmental impact of electricity was evaluated for operation times of 12 and 24 h and was found to fall within the rage of scientific literature data.

When calculating the specific environmental impacts of electricity in this system (which does not consume any fuel), the predominant contributions are from the environmental impact rate of components, exergy destruction rate (included in the total environmental impact rate) and exergy efficiency.

A sensitivity analysis showed the effect of operation time on the performance of the power plant and on the specific environmental impact of electricity, highlighting the importance of the net power and exergy efficiency in the environmental performance.

Further research can focus on employing the environmental impact rate of the components presented by [28], which addresses a solar-geothermal system and presented the highest values obtained in the scientific literature.

Acknowledgments The authors wish to thank the Coordination for the Improvement of Higher Education Personnel (CAPES) for the MSc. Scholarship.

References

1. Gładysz P, Ziebik A (2016) Environmental analysis of bio-CCS in an integrated oxy-fuel combustion power plant with CO_2 transport and storage. Biomass Bioenerg 85:109–118. https://doi.org/10.1016/j.biombioe.2015.12.008
2. Singh B, Strømman AH, Hertwich E (2011) Life cycle assessment of natural gas combined cycle power plant with post-combustion carbon capture, transport and storage. Int J Greenh Gas Contr 5:457–466. https://doi.org/10.1016/j.ijggc.2010.03.006
3. Cavalcanti EJC, Carvalho MA (2019) Exergoenvironmental results of a eucalyptus biomass-fired power plant. Energy 189:116188. https://doi.org/10.1016/j.energy.2019.116188
4. Bravo Y, Carvalho M, Serra LM, Monne C, Alonso S, Moreno S, Munõz M (2012) Environmental evaluation of dish-Stirling technology for power generation. Sol Energy 86:2811–2825. https://doi.org/10.1016/j.solener.2012.06.019
5. Behar O, Khellaf A, Mohammedi KA (2013) Review of studies on central receiver solar thermal power plants. Renew Sustain Energy Rev 23:12–39. https://doi.org/10.1016/j.rser.2013.02.017
6. González-Gómez PA, Gómez-Hernández J, Briongos JV, Santana D (2017) Thermo-economic optimization of molten salt steam generators. Energy Conver Manag 146:228–243. https://doi.org/10.1016/j.enconman.2017.05.027
7. Bejan A, Tsatsaronis G, Moran MJ (1996) Thermal design and optimization, 1st edn. Wiley, New York
8. Zare V, Hasanzadeh M (2016) Energy and exergy analysis of a closed Brayton cycle-based combined cycle for solar power tower plants. Energy Convers Manag 128:227–237. https://doi.org/10.1016/j.enconman.2016.09.080
9. Okonkwo EC, Okwose CF, Abid M, Ratlamwala TAH (2018) Second-law analysis and exergoeconomics optimization of a solar tower-driven combined-cycle power plant using supercritical CO_2. J Energy Eng 144(3):04018021–040180212. https://doi.org/10.1061/(asce)ey.1943-7897.0000534
10. Serrano-Sanchez C, Olmeda-Delgado M, Petrakopoulou F (2019) Exergy and economic evaluation of a hybrid power plant coupling coal with solar energy. Appl Sci 9(5):850–869. https://doi.org/10.3390/app9050850
11. Gómez-Hernández J, González-Gómez PA, Briongos JV, Santana D (2018) Influence of the steam generator on the exergetic and exergoeconomic analysis of solar tower plants. Energy 145:313–328. https://doi.org/10.1016/j.energy.2017.12.129
12. Demir ME, Dincer I (2017) Development and analysis of a new integrated solar energy system with thermal storage for fresh water and power production. Int J Energy Res 42(9):2864–2874. https://doi.org/10.1002/er.3846
13. Bonforte G, Buchgeister J, Manfrida G, Petela K (2018) Exergoeconomic and exergoenvironmental analysis of an integrated solar gas turbine/combined cycle power plant. Energy 156:352–359. https://doi.org/10.1016/j.energy.2018.05.080
14. Nemati A, Nami H, Yari M (2018) Assessment of different configurations of solar energy driven organic flash cycles (OFCs) via exergy and exergoeconomic methodologies. Renew Energy 115:1231–1248. https://doi.org/10.1016/j.renene.2017.08.096
15. Baghernejad A, Yaghoubi M, Jafarpur K (2016) Exergoeconomic comparison of three novel trigeneration systems using SOFC, biomass and solar energies. Appl Therm Eng 104:534–555. https://doi.org/10.1016/j.applthermaleng.2016.05.032
16. Liu H, Zhai R, Patchigolla K, Turner P, Yang Y (2020) Performance analysis of a novel combined solar trough and tower aided coal-fired power generation system. Energy 201:117597. https://doi.org/10.1016/j.energy.2020.117597
17. Yilmaz F, Ozturk M, Selbas R (2020) Development and performance analysis of a new solar tower and high temperature steam electrolyzer hybrid integrated plant. Int J Hydrogen Energy 45:5668–5686. https://doi.org/10.1016/j.ijhydene.2019.03.061
18. Boukelia TE, Bouraoui A, Laouafi A, Djimli S, Kabar Y (2020) 3E (Energy-Exergy-Economic) comparative study of integrating wet and dry cooling systems in solar tower power plants. Energy 200:117567. https://doi.org/10.1016/j.energy.2020.117567
19. Meyer L, Tsatsaronis G, Buchgeister J, Schebek L (2009) Exergoenvironmental analysis for evaluation of the environmental impact of energy conversion systems. Energy 34(1):75–89
20. Cavalcanti EJC (2017) Exergoeconomic and exergoenvironmental analyses of an integrated solar combined cycle system. Renew Sustain Energy Rev 67:507–519
21. Montazerinejad H, Ahmadi P, Montazerinejad Z (2019) Advanced exergy, exergoeconomic and exergoenvironmental analyses of a solar based trigeneration energy system. Appl Therm Eng 152:666–685. https://doi.org/10.1016/j.energy.2008.07.018
22. Boyaghchi FA, Chavoshi M (2017) Multi-criteria optimization of a micro solar-geothermal CCHP system applying water/CuO nanofluid based on exergy, exergoeconomic and exergoenvironmental concepts. Appl Therm Eng 112:660–675. https://doi.org/10.1016/j.applthermaleng.2016.10.139

23. Tehrani SSM, Taylor RA, Nithyanandam K, Ghazani AS (2017) Annual comparative performance and cost analysis of high temperature, sensible thermal energy storage systems integrated with a concentrated solar power plant. Sol Energy 153:153–172. https://doi.org/10.1016/j.solener.2017.05.044
24. Peiró G, Prieto C, Gasia J, Jové A, Miró L, Cabeza LF (2018) Two-tank molten salts thermal energy storage system for solar power plants at pilot plant scale: lessons learnt and recommendations for its design, start-up and operation. Renew Energy 121:236–248. https://doi.org/10.1016/j.renene.2018.01.026
25. Oró E, Gil A, Gracia A, Boer D, Cabeza LF (2012) Comparative life cycle assessment of thermal energy storage systems for solar power plants. Renew Energy 44:166–173. https://doi.org/10.1016/j.renene.2012.01.008
26. Cavalcanti EJC, Motta PH (2015) Exergoeconomic analysis of a solar- powered/fuel assisted Rankine cycle for power generation. Energy 88:555–562. https://doi.org/10.1016/j.energy.2015.05.081
27. Rodriguez-Sanchez MR, Sanchez-Gonzalez A, Marugan-Cruz C, Santana D (2015) Flow patterns of external solar receivers. Sol Energy 122:940–953. https://doi.org/10.1016/j.solener.2015.10.025
28. Ferri R, Cammi A, Mazzei D (2008) Molten salt mixture properties in RELAP5 code for thermodynamic solar applications. Int J Therm Sci 47(12):1676–1687. https://doi.org/10.1016/j.ijthermalsci.2008.01.007
29. Lazzaretto A, Tsatsaronis G (2006) SPECO: a systematic and general methodology for calculating efficiencies and costs in thermal systems. Energy 31:1257–1289. https://doi.org/10.1016/j.energy.2005.03.011Get
30. ISO 14040 (2006) Environmental management - life cycle assessment–requirements and guidelines (2006) Geneva: International Organization for Standardization (ISO)
31. Goedkoop M, Effing S, Collignon M (2000) Eco-indicator 99/ manual for designers–a damage oriented method for life cycle impact assessment, 2nd edn. Ministry of Housing, Spatial Planning and the Environment
32. Hosseini SE, Barzegaravval H, Ganjehkaviri A, Wahid MA, Jaafar MNM (2017) Modelling and exergoeconomic-environmental analysis of combined cycle power generation system using flameless burner for steam generation. Energy Convers Manag 135:362–372. https://doi.org/10.1016/j.enconman.2017.01.001
33. Ma Y, Morozyuk T, Liu M, Yan J, Liu J (2019) Optimal integration of recompression supercritical CO_2 Brayton cycle with main compression intercooling in solar power tower system based on exergoeconomic approach. Appl Energy 242:1134–1154. https://doi.org/10.1016/j.apenergy.2019.03.155
34. Wellmann J, Meyer-kahlen B, Morosuk T (2018) Exergoeconomic evaluation of a CSP plant in combination with a desalination unit. Renew Energy 128:586–602. https://doi.org/10.1016/j.renene.2017.11.070
35. ECOINVENT (2018) Database. software SimaPro 2018, version 8.5.2.0. Pre-Sustainability. http://www.ecoinvent.org/. Accessed 18 Apr 2018
36. Cavalcanti EJC, Carvalho M, Ochoa AAV (2019) Exergoeconomic and exergoenvironmental comparisons of diesel-biodiesel blends in a stationary engine at variable loads. Energy Convers Manag 183:450–461. https://doi.org/10.1016/j.enconman.2018.12.113
37. Aghbashlo M, Tabatabaei M, Soltanian S, Ghanavati H (2019) Biopower and biofertilizer production from organic municipal solid waste: An exergoenvironmental analysis. Renew Energy 143:64–76. https://doi.org/10.1016/j.renene.2019.04.109